Available online at www.sciencedirect.com
SCIENCE DIRECT®
PHOTONICS AND NANOSTRUCTURES Fundamentals and Applications
Photonics and Nanostructures – Fundamentals and Applications 2 (2004) 1–10
www.elsevier.com/locate/photonics

# Modal behavior of single-line photonic crystal guiding structures on InP substrate

A. Talneau [a,*], M. Mulot [b], S. Anand [b], S. Olivier [c], M. Agio [d,e], M. Kafesaki [f], C.M. Soukoulis [d,f]

[a] CNRS/Laboratoire de Photonique et de Nanostructures, Route de Nozay, F-91460 Marcoussis, France
[b] Department of Microelectronics and Information Technology, Royal Institute of Technology, S-164 40 Kista, Sweden
[c] Laboratoire de Physique de la Matière Condensée, Ecole Polytechnique, UMR 7643, CNRS 91128 Palaiseau, France
[d] INFM-Dipartimento di Fisica "A. Volta", Università di Pavia, via Bassi, 6 I-27100 Pavia, Italy
[e] Ames Laboratory and Department of Physics and Astronomy, Iowa State University, Ames, IA 50011, USA
[f] Research Center of Crete, IESL-FORTH, Heraklion, Crete, Greece

Received 23 July 2003; received in revised form 17 November 2003; accepted 20 November 2003

**Abstract**

We have experimentally investigated the modal behaviour and the polarization dependence of the transmission through single-missing-row photonic crystal (PC) straight guides, bends and combiners, fabricated on InP substrate. A photonic crystal-based taper has been included to funnel light in these strongly confined structures. Two-dimensional finite-difference time-domain simulations have been performed and favorably compared with the measurements. It is found that the scattering process occurring at a bend/combiner transition plays a key role on the overall transmission.


*PACS:* 42.82

*Keywords:* Photonic crystals; Guiding structures; Photonic integrated circuits

## 1. Introduction

In-plane integrated optics could take advantage of the specific modal behaviour of light in a photonic crystal (PC) environment. We propose here to draw general design rules for a full PC-based photonic integrated circuit, relying on the understanding of the modal behaviour of PC-based guiding structures and on quantitative transmission performances.

Strong-confinement single-missing-row photonic crystal waveguides (PCW) can be credible candidates for photonic integrated circuits, provided they demonstrate low propagation losses in straight guides and high transmission through bends and combiners. A single-missing-row PCW, named W1, is obtained by removing an entire row of holes in a uniform photonic crystal. The W1 PCW attracts interest as it supports a single spatially even mode on most of the photonic band gap. Such a system has been thoroughly investigated on membrane structures [1–7], where lossless modes exist below the light cone. A membrane-based structure is a very interesting object of study, but

* Corresponding author. Tel.: +33-169-636146; fax: +33-169-636006.
*E-mail address:* anne.talneau@lpn.cnrs.fr (A. Talneau).

1569-4410/$ – see front matter © 2003 Elsevier B.V. All rights reserved.
doi:10.1016/j.photonics.2003.11.002

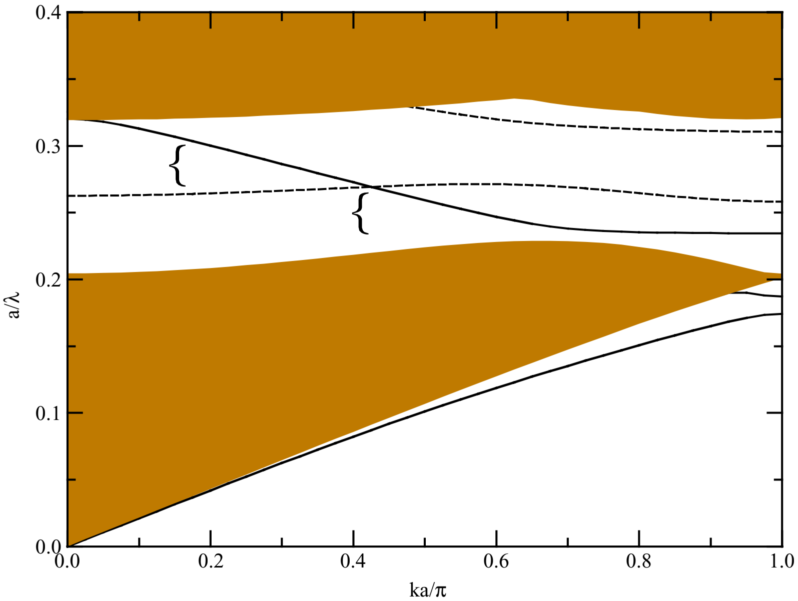


Fig. 1. Dispersion diagram of a W1 PCW ($f = 40\%$) along the ΓK direction. The two frequency domains investigated $u = 0.28$ and $u = 0.24$ are shown by braces. Solid (dashed) lines represent spatially even (odd) TE guided modes.

injecting light in the structure still remains challenging [8]; furthermore, for any in-plane optical function, the design will probably break the PC translational symmetry, then light is not transmitted anymore on lossless modes.

The present work addresses designs which could be compatible with active PC-based structures as emitters, modulators and amplifiers in the 1.55 μm wavelength domain. Our PC is a triangular lattice of holes etched through a weak confinement InP-based planar waveguide. A W1 PCW is obtained by removing a single row in the ΓK crystal direction; no hole-size variations within the guide or on the first inner row are investigated here. In such a system, all modes sustained by a line defect within the photonic gap lie above the light line and thus exhibit propagation losses. Fig. 1 shows the dispersion curve for the W1 PCW for air filling factor $f = 40\%$; $u = a/\lambda$ is the reduced frequency, $a$ being the lattice constant and $\lambda$ the wavelength. Two frequency domains are of interest: $u = 0.28$ and $u = 0.24$, above and below the spatially odd mode, respectively. The W1 PCW, a strong-confinement structure, suffers from poor coupling to any classical InP compatible ridge guide. We have designed and measured a PC-based taper [9] that overcomes this difficulty and allows us to address the modal properties of PC bends and splitters.

Polarisation conversion is a severe drawback of index-guided sharp bends [10], and will always limit the size reduction of photonic integrated circuits based on the classical index-contrast guiding mechanism. Here, we also present measurements on PCW W1-based sharp bends, which demonstrate that polarization conversion is suppressed to better than 17 dB. We then demonstrate on a two-to-one combiner the advantage of additional small holes in the combining region, which prevent excitation of higher order modes. The 3 dB intrinsic limit of a two-branch symmetric combiner is reached in this design. These measurements are in agreement with two-dimensional (2D) finite-difference time-domain (FDTD) simulations.

## 2. General description of sample fabrication and design

The PCW is obtained from a 2D PC consisting of a triangular array of holes drilled in a 500 nm thick

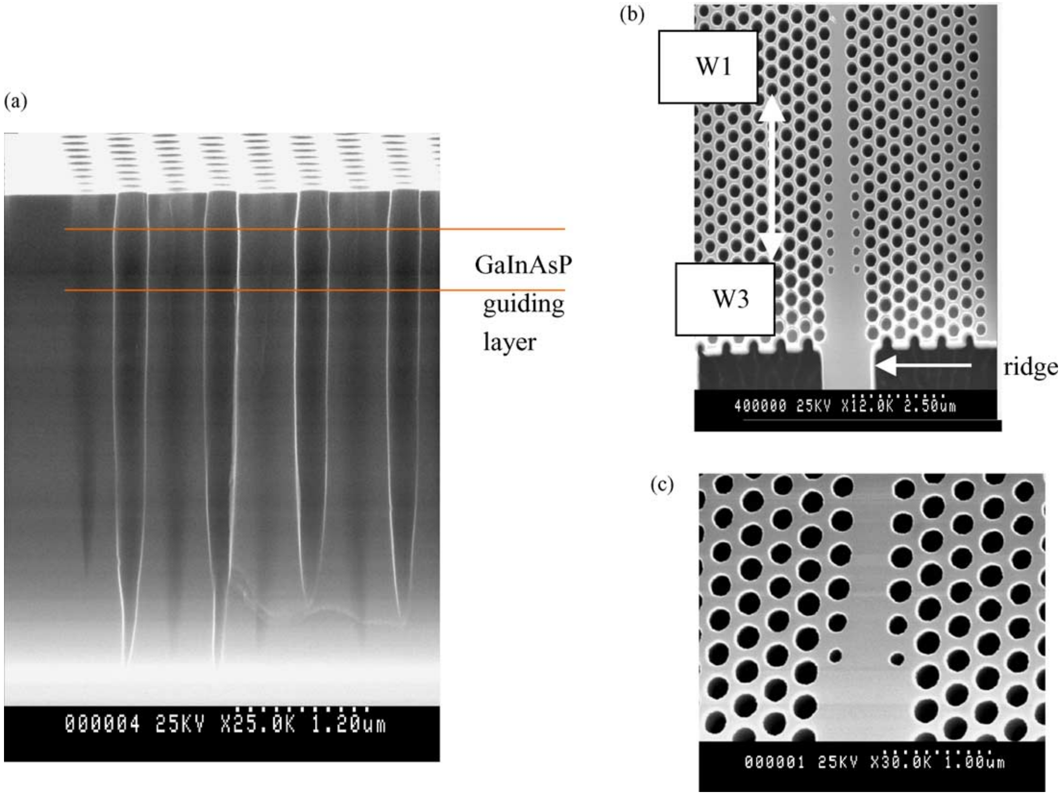


Fig. 2. (a) CAIBE etched PC in the GaInAsP layer. (b) Top view of the ridge access guide entering the W3, and then the 10-rows-long taper fabricated in the $u = 0.28$ domain. (c) Top view of the four-rows-long taper, for the $u = 0.24$ domain.

GaInAsP confining layer, by Chemically Assisted Ion Beam Etching (CAIBE), using $Ar/Cl_2$ chemistry [11]. In Fig. 2(a), a micrograph of the structure shows holes deeper than 3 μm for an air-filling factor $f = 40\%$. For a reproducible coupling of light in and out of the PC section, the W1 PCW is inserted in between two mono-mode ridge access guides, limited by cleaved facets. A general view of the transition between a ridge access guide and a PC guide is shown on Fig. 2(b). A tapered section based on a gradual variation of hole sizes and depths [9] is inserted at every ridge/W1 transition. To address the $u = 0.28$ frequency domain mode ($\lambda = 1.5$ μm, $a = 450$ nm), we have fabricated a taper distributed on 10 rows as visible in Fig. 2(b). As discussed in [12], the taper can be much shorter, provided that the first hole is very small. An attempt to fabricate such a small hole is shown on Fig. 2(c), where the taper is distributed on four rows, used for operation in the frequency domain $u = 0.24$ ($\lambda = 1.5$ μm, $a = 360$ nm).

## 3. Measurements

Measurements are performed in TE-polarization, on a 1410–1590 nm wavelength span, covered by two polarization-maintaining-output tunable-laser sources. TE-polarization corresponds to the electric field perpendicular to the holes' axis. Laser light is injected in the ridge access guide using a micro-lens fiber whose waist is 2 μm, matching as much as possible the size of the mode supported by the ridge access guide. The light is collected through a fiber of the same type; by interposing an analyzer, we study the polarization behavior of the PC structure under test. The polarization rejection of the tunable sources is −17 dB.

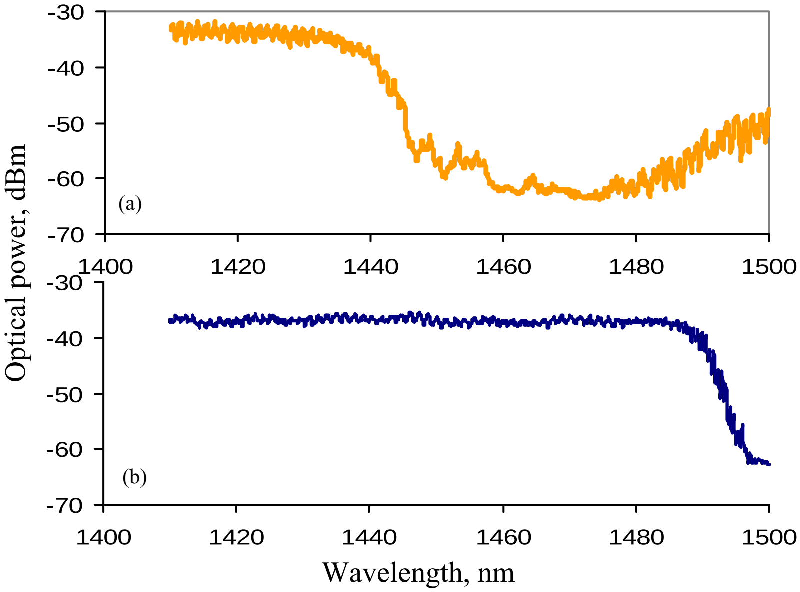


Fig. 3. Transmission spectra through W1 PCWs exhibiting a cut-off (a) $f = 40\%$, (b) $f = 34\%$.

## 4. Transmission through straight W1 guides and PC taper

Previous investigations concerned the frequency domain $u = 0.28$, requiring, for the wavelength domain of 1410–1590 nm, a PC period $a = 450$ nm and hole diameters around 300 nm to obtain an air filling factor of 40%. Propagation losses of 600 dB/cm in a W1 PCW have been measured using the Fabry–Perot resonance method, while the taper efficiency was limited to 50%, due to the too large size of the first hole [13].

An improved fabrication process allows the investigation of the $u = 0.24$ frequency domain, which requires smaller holes ($a = 360$ nm, hole diameter $=$ 230 nm). Referring to Fig. 1, when the wavelength increases, one can follow the spatially even mode to slow-down to its cut-off at $k = \pi/a$. This feature is clearly visible in the transmission spectrum of Fig. 3(b). The very sharp variation of the transmission, more than 30 dB on a 10 nm range, allows an accurate estimate of the air filling factor $f$ ($\delta f < 1\%$), as the $u$ value of the cut-off is very dependent on $f$. Using the effective index model in a 2D simulation, as proposed in [14], we find $f = 34\%$. For the structure of Fig. 3(a), the cut-off occurs at 1440 nm, corresponding to $f = 40\%$. One can see here the strongly attenuated transmission after the cut-off, where no modes exist within the gap; then, starting from 1480 nm, the transmission increases because the light is now guided through the modes of the PC dielectric band. The sharp cut-off of the spatially even mode could be advantageously used for filtering applications.

The propagation losses measured in the $u = 0.24$ frequency domain are as large as 1000 dB/cm, larger than the 600 dB/cm measured in the $u = 0.28$ domain. This is related to the fact that the mode in the $u = 0.24$ domain has a larger extent within the holes. Due to the improved process, which now allows hole fabrication with a diameter as low as 100 nm, the taper shown in Fig. 2(c) achieves a flat transmission of 70% on the whole wavelength domain 1410–490 nm, visible on Fig. 3(b). For PC-based PICs, one would now give up the W1 PCW, and use a wider PCW, which exhibit less loss. But, one must wonder what happens in a bend.

## 5. Polarization behavior of double-bends: the multimode W3 PCW versus the monomode W1 PCW

As we stated before, polarization is a severe drawback in sharp bends based on the total reflection guiding mechanism. We investigate how polarization conversion is of concern here, comparing the transmission through the W3 multimode PCW versus the W1 monomode PCW. This comparison is performed in the $u = 0.28$ frequency domain.

Previous measurements [15] have pointed out low losses for wide and thus multi-mode straight PCWs. However, it is clear that, at a bend, multi-mode ports lead to some amount of mode scrambling, preventing device cascadability. Nevertheless, it has been demonstrated that moving holes at the corner of these wide PCW bends may increase transmission [16,17].

Fig. 4(a) shows the TE-polarization dispersion curve for a three-missing-rows straight PCW, named W3, and the SEM picture of a W3 double bend with three holes-moved at each bend. Fig. 4(b) displays the TE-polarization dispersion curve for the W1 PCW and the SEM picture of a W1 double-bend with one hole-moved at the corners. The frequency domain of interest is around $u = 0.28$, where the W1 PCW is mono-mode. The ridge access guides can support a single TE mode and a single TM mode; the injected light is TE polarized. The transmitted spectrum is filtered through an analyzer in order to measure both the TE and the TM components at the output of the PCW double bend. On both Fig. 5(a) and (b), the straight PCW is plotted as a reference. For the W3 double-bend (Fig. 5(a)) the TM level is found to be

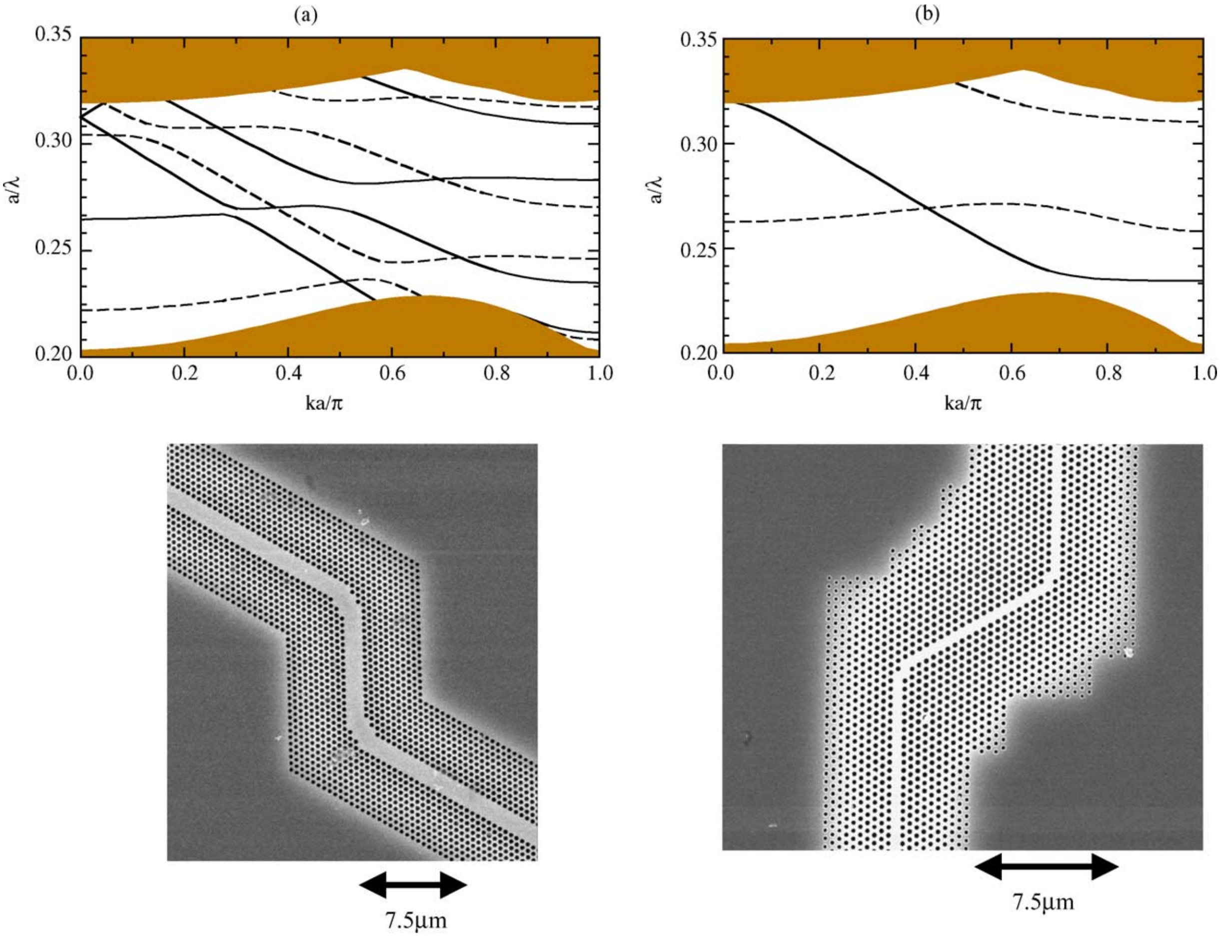


Fig. 4. Top views of double-bends and dispersion curves of the PCW ($f = 40\%$), (a) W3 and (b) W1. Solid (dashed) lines represent spatially even (odd) TE guided modes.

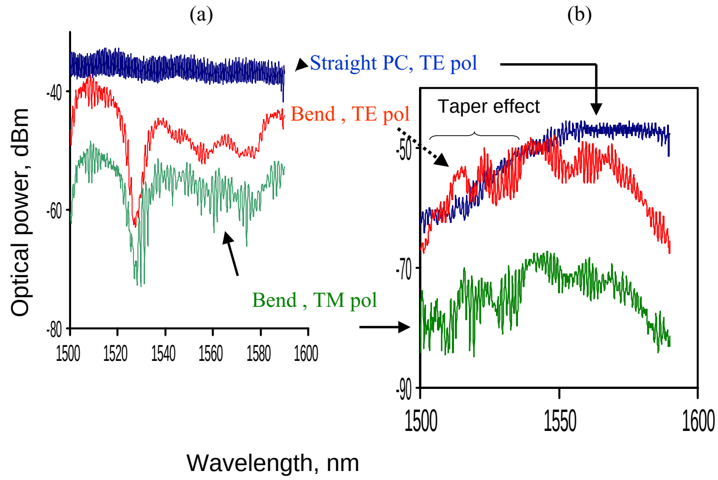


Fig. 5. Polarisation dependent transmission spectra in the $u = 0.28$ domain for (a) W3 double-bends and (b) W1double-bends ($f = 40\%$).

10 dB below the TE, whereas for the W1 double-bend (Fig. 5(b)) the TM level is 17 dB below the TE the polarization selectivity of the external tunable source. Clearly no measurable polarization conversion occurs in the W1 double-bend, whereas some conversion has occurred in the W3-based double bend. The scattering process at the bend is also responsible for this different behavior: the W3 PCW is a wide guide and even being excited on its fundamental mode, a large number of modes exist in the bend section. For some of these modes, polarization conversion occurs due to the continuity conditions, in the same way as it does in purely index-guided sharp bends [10]. In the case of the W1 PCW, we have already seen that a very reduced number of modes exist in the bend section (two in the $u = 0.28$ domain), so that polarization conversion is limited.

## 6. Modal behavior of a W1 double-bend

We then investigate the transmission through a W1 double bend, as any in-plane optical function would require bending the guide. We focused on a one-hole-moved W1 design (see SEM photograph of Fig. 6(b)), and compared the two frequency domains $u = 0.28$ and $u = 0.24$. In the $u$=0.28 domain, losses are at least 3 dB per bend (1550–1570 nm) as visible in Fig. 5(b), in the $u = 0.24$ domain, losses are reduced to 1 dB per bend on a 40 nm range, as seen in Fig. 6(a) when comparing the straight W1 PCW to the double bend. Since the design is the same, one-hole-moved in both frequencies, the reason for reduced bend transmission in the $u = 0.28$ domain can be explained as follows [2].

The bend transition is, in fact, a resonant scattering process, as clearly described in [18]. The mode propagating in the straight guide is scattered into the modes supported by the bend section: some are partly reflected and transmitted; some could be more efficiently coupled to radiation modes. Following [2], the bend region can be modeled as an infinite PCW in the ΓM direction, see Fig. 6(b), whose dispersion relation is shown in Fig. 6(c). We find two guided modes in the $u = 0.28$ frequency domain and only one in the $u = 0.24$ domain. Therefore, in the $u = 0.28$ domain, the single mode of the W1 PCW is scattered into two modes, so that part of the power is lost via the second mode. This modal scattering does not occur in the $u = 0.24$ domain, which remains mono-mode also in the bend section, thus ensuring a better transmission. One can also notice that the mode cut-off for the straight guide occurs at a wavelength around 1570 nm; whereas, it occurs at a lower wavelength, around 1554 nm, for the double-bend. The samples were fabricated during the same run, and very close to each other; technological inhomogeneities cannot be responsible for this shift. We propose that the shift

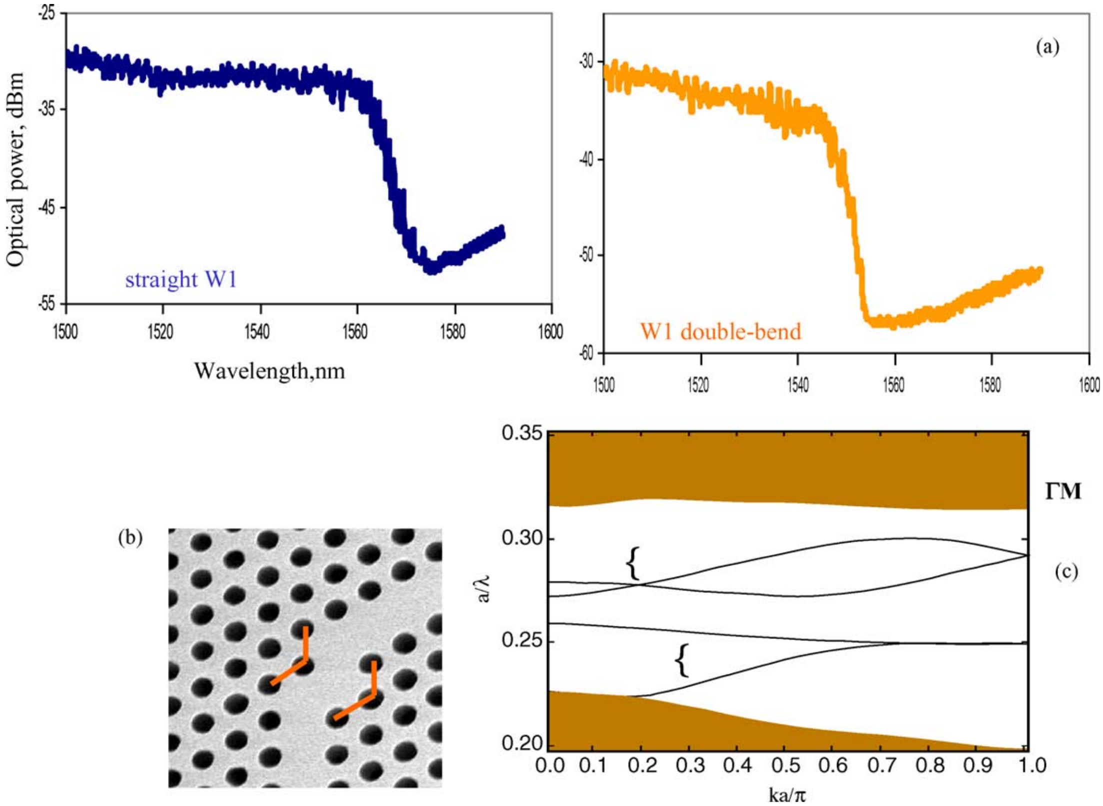


Fig. 6. (a) Transmission spectra in the $u = 0.24$ domain through a W1 double bend (right), the straight guide is plotted as a reference (left). (b) Enlarged SEM top view of a one-hole-moved bend. (c) Dispersion curve of a W1 PCW in the ΓM direction ($f = 40\%$).

of the mode cut-off shows that the bend efficiency is strongly affected when the mode evolves towards its zero group velocity limit.

A PIC design would then take advantage of the W1 bend, which does not demonstrate polarisation conversion, and can transmit 90% in the $u = 0.24$ frequency domain. In the next section, we investigate W1-based more complex structures, namely branching structures.

## 7. Combiner without (case a) and with (case b) additional holes

Integrated circuits will require combiners and splitters to implement, for example, interferometric functions (Mach-Zehnder), or to realise WDM integrated sources. W1 is still our candidate due to the polarisation advantage in the bend. We investigated *Y*-geometry based combiners as presented in the inset of Fig. 7; each W1 PCW has a PC taper access. Such a *Y*-design will inherently demonstrate 3 dB loss for non-coherent sources. But on the other hand, it allows a wide transmission bandwidth, which is of interest in WDM sources, or when using the Mach-Zehnder interferometer as a wavelength converter.

We rely on 2D FDTD calculations for the designs. We include a phenomenological parameter $\varepsilon_{im}$ describing radiation loss in the third dimension, despite the 2D simulation model [19].

We first investigated the $u = 0.28$ domain, and tried to improve the junction transmission through the addition of small holes. We present here two interesting designs of the "enlarged" combining section, zoomed on the micrographs of Fig. 7(a) and (b). For Fig. 7(a), the combining section, locally larger than W1, allows

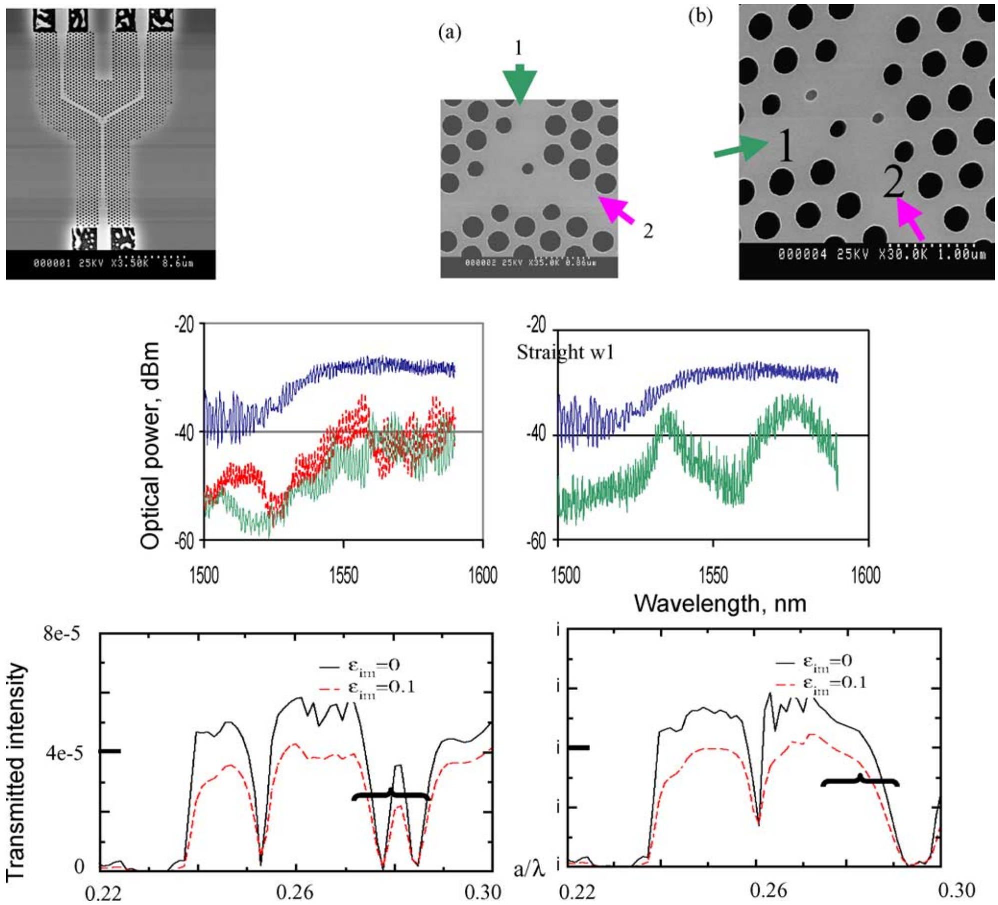


Fig. 7. W1-based combiners for operation in the $u = 0.28$ domain. (a) No hole added and (b) two small holes added. Top: enlarged SEM view of the combining region. Middle: measured transmission spectra for both outputs of the combiner, the straight W1 is plotted as a reference. Bottom: FDTD simulation $\varepsilon_{\rm im} = 0$ (solid line), $\varepsilon_{\rm im} = 0.1$ (dotted line). The operating frequnecy domain is shown by a brace.

higher-order modes to be excited; whereas, for Fig. 7(b), two small holes have been added to prevent such an effect. Measurements of transmission through both combiners are presented in Fig. 7 (middle), using the straight guide as a reference. One must consider that the absolute transmission level through the whole combiner includes the combining region and one 60° bend. As the bend is the same in both cases, this allows us to conclude that including these two small holes increases the combiner transmission by 5 dB. Some internal reflections are still visible through large oscillations in Fig. 7(b) and could be limited by means of additional holes along the straight guide as proposed by Boscolo et al. in [20]. The discrepancy visible between the two inputs, see Fig. 7(b), is attributed to the different sizes of the two additional small holes. These measurements are in agreement with FDTD simulations plotted in Fig. 7 (bottom) for two loss parameters: $\varepsilon_{\rm im} = 0$ (solid line) and $\varepsilon_{\rm im} = 0.1$ (dotted line). Within the operating frequency domain around $u = 0.28$, case (b) is more favourable than case (a).

For an overall better transmission, we then move to the $u = 0.24$ frequency domain, where the W1 bend has better performance. Also, as we learned previously it is difficult to fabricate two additional holes of the exact same size. We investigated designs reducing the combining region and including holes of the same size as the holes of the PC-matrix . We present

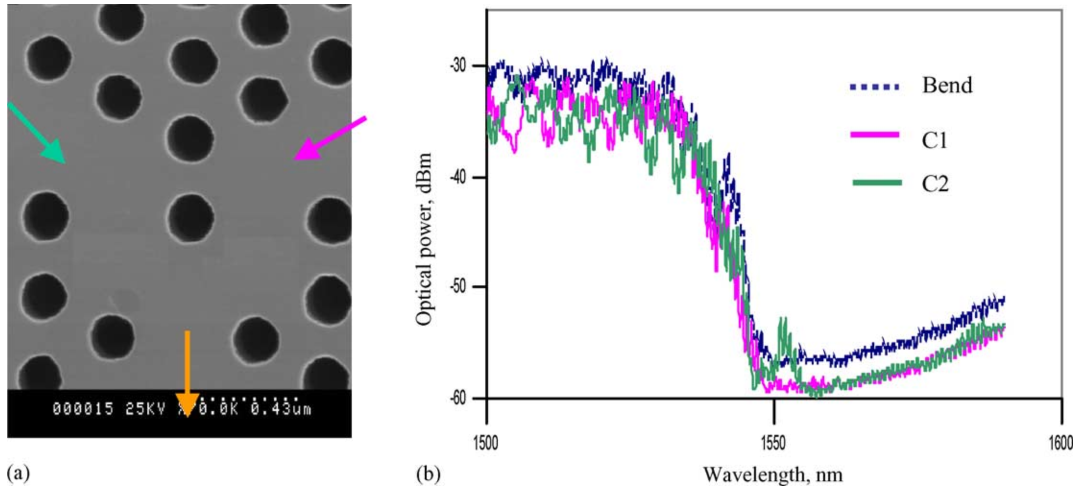


Fig. 8. W1-based combiner for operation in the $u = 0.24$ domain: (a) SEM top view of the combining region and (b) transmission spectra for the two outputs (solid lines). The double-bend is plotted as a reference (dotted line).

the results of a combining region reduced by adding a single hole having the size of the holes of the PC-matrix, see Fig. 8(a). Transmission spectra for the two inputs are plotted in Fig. 8(b), choosing the double-bend as a reference. Despite some residual reflections, the transmission is close to the intrinsic 3 dB limit of any two to one non-resonant branching geometry, between similar mono-mode ports. The transmission on both inputs shows again the cut-off of the W1 mode. The spectral position of the cut-off for the combiner is very close to the one for the double-bend, i.e. blue-shifted with respect to the straight guide. This similarity could be explained by the fact that the zero group velocity mode moves across the bend and the combiner. The advantage of such a PC combiner is the compactness and the absence of polarization mixing. Using a single additional hole of the same size makes the fabrication more reliable and no asymmetry is visible between the two inputs.

## 8. Discussion

From the insight gained through these measurements, the bend performances appear to be better in the lower frequency domain $u = 0.24$, rather than in the higher frequency domain $u = 0.28$. The fabrication cannot be the reason for this difference, as all samples are CAIBE etched, with at least 3 μm deep holes. Small holes (for the $u = 0.24$ domain) are of course more subject to imperfections. This difference could originate from the scattering process that occurs when the translational symmetry is broken. This process re-distributes the wave vector $\boldsymbol{k}$ of the incoming mode on all the $\boldsymbol{k}$ vectors allowed in the bend/combiner section. The smaller the number of modes in this section, the better transmission; this is the advantage of the $u = 0.24$ domain versus the $u = 0.28$ domain.

Going to single mode W1 PCW-based structures, one must remember that the propagation losses of the spatially even mode are larger in the $u = 0.24$ domain than in the higher frequency domain. These established facts strengthen our earlier proposal [9] to find the optimal trade-off between propagation losses and bending/combining geometries, by combining a wide PCW in straight sections and W1-based bends/combiners taking advantage of a tapering transition in-between.

## 9. Conclusion

The propagation through strongly confined PC straight guides, bends and combiners has been investigated. We explained these experimental trends with the scattering process occurring at each bend/combiner transition. No polarization conversion occurs in W1-based PC bends, which demonstrates the potential for this guiding geometry for high compactness photonic integrated circuits. Additional holes are shown to play an important role in combining geometries that demonstrate performance comparable to classical *Y* junctions on a much shorter length. The W1 PCW seems very promising, but still suffers from high linear losses compared to wider PC guides. The PC-based taper used here could overcome this problem by allowing propagation in wide guides that become W1 mono-mode guides whenever necessary.

## Acknowledgements

This work is supported by the IST PCIC project. A. Talneau acknowledges the Région Ile de France SESAME project no. 1377 and the Conseil Général de l'Essone.

## References

[1] T. Baba, A. Motegi, T. Iwai, N. Fukaya, Y. Watanabe, A. Sakai, IEEE J. Quantum. Electron. 38 (2002) 743–752.
[2] A. Chutinan, M. Okano, S. Noda, Appl. Phys. Lett. 80 (2002) 1698–1700.
[3] S. Yamada, T. Koyama, Y. Katayama, J. Appl. Phys. 89 (2001) 855–858.
[4] E. Chow, S.Y. Lin, J.R. Wendt, S.G. Johson, J.D. Joannopoulos, Opt. Lett. 26 (2001) 286–288.
[5] M. Loncar, D. Nedeljkovic, . Doll, J. Vuckovic, A. Scherer, T. Paersall, Appl. Phys. Lett. 77 (2000) 1937–1939.
[6] M. Notomi, A. Shinya, K. Yamada, J. Takahashi, C. Takahashi, I. Yokohama, Elec. Lett. 37 (2001) 293–295.
[7] Y. Sugimoto, N. Ikeda, N. Carlsson, K. Asakawa, N. Kawai, K. Inoue, Appl. Phys. Lett. 79 (2001) 4286–4288.
[8] V. Berger, I. Pavel, E. Ducloux, F. Lafon, J. Appl. Phys. 82 (1997) 5300–5304.
[9] A. Talneau, Ph. Lalanne, M. Agio, C.M. Soukoulis, Opt. Lett. 27 (2002) 1522–1524.
[10] C. van Dam, L.H. Spiekman, F.P.G.M. van Ham, F.H. Groen, J.J.G.M. van der Tol, I. Moerman, W.W. Pascher, M. Hamamcher, H. Heidrich, C.M. Weinert, M.K. Smit, IEEE Phot. Technol. Lett. 8 (1996) 1346–1348.
[11] M. Mulot, S. Anand, C.F. Carlström, M. Swillo, A. Talneau, Phys. Scr. T101 (2002) 106–109.
[12] Ph. Lalanne, A. Talneau, Opt. Express 10 (2002) 354.
[13] A. Talneau, M. Mulot, S. Anand, Ph. Lalanne, Appl. Phys. Lett. 82 (2003) 2577–2579.
[14] M. Qiu, Appl. Phys. Lett. 81 (2002) 1163–1165.
[15] A. Talneau, L. Legouezigou, N. Bouadma, Opt. Lett. 26 (2001) 1259–1261.
[16] A. Talneau, L. Legouezigou, N. Bouadma, M. Agio, Appl. Phys. Lett. 80 (2002) 547–549.
[17] S. Olivier, H. Benisty, C. Weisbuch, C.J.M. Smith, T.F. Krauss, R. Houdré, U. Oesterle, IEEE, J. Lightwave. Technol. 20 (2002) 1198–1203.
[18] A. Mekis, J.C. Chen, I. Kurland, S. Fan, P.R. Villeneuve, J.D. Joannopoulos, Phys. Rev. Lett. 77 (1996) 3787–3790.
[19] H. Benisty, D. Labilloy, C. Weisbuch, C.J.M. Smith, T.F. Krauss, D. Cassagne, A. Beraud, C. Jouanin, Appl. Phys. Lett. 76 (2000) 532–534.
[20] S. Boscolo, M. Midrio, T.F. Krauss, Opt. Lett. 27 (2002) 1001–1003.